**Variational demonstration: AMSU and ATMS water vapor estimates**

Understand the variational approach through a demonstration…

$$\hat{x} = x_a + \left(K^T S_\varepsilon^{-1} K + S_a^{-1}\right)^{-1} K^T S_\varepsilon^{-1}\left(y - K x_a\right) \qquad \text{(1 linear)}$$

$$x_{i+1} = x_i + \left(S_a^{-1} + K_i^T S_\varepsilon^{-1} K_i\right)^{-1}\left[K_i^T S_\varepsilon^{-1}\left(y - F\left(x_i\right)\right) - S_a^{-1}\left(x_i - x_a\right)\right] \qquad \text{(1 nonlinear)}$$

Consider the Advanced Microwave Sounding Unit, AMSU. AMSU-B has three 183 GHz channels at 183.31 $\pm$1, $\pm$3 , $\pm$7 GHz. This instrument is used to profile atmospheric water. We will also examine the impact of additional frequencies

183.31,183.81,184.31,185.31,186.31,188.31,190.31

These three channels provide insufficient information to profile water vapor very well by themselves. However, it is useful information for improving *apriori* water vapor profile information.

So we apply the Bayesian variational approach via equation (1) to combine the AMSU data constraints with apriori water vapor estimates to improve our water vapor estimates.

**State and measurement vectors**

To simplify things, as the state vector, we use only the water vapor partial pressures at the number of altitudes in the atmospheric state. We don't include temperature and other atmospheric variables or surface properties in the state vector to simplify the problem and essentially estimate the maximum effect the radiance measurements can have on the estimated water vapor field.

$$x = \begin{bmatrix} P_w\left(z_n\right) \\ \vdots \\ P_w\left(z_2\right) \\ P_w\left(z_1\right) \end{bmatrix} \qquad (2)$$

The measurement vector, *y*, consists of the series of measurements of radiances near the 183 GHz water line.

$$y = \begin{bmatrix} L\left(f_m\right) \\ \vdots \\ L\left(f_2\right) \\ L\left(f_1\right) \end{bmatrix} \qquad (3)$$

**Forward Calculation**

First, we create a temperature-pressure structure.

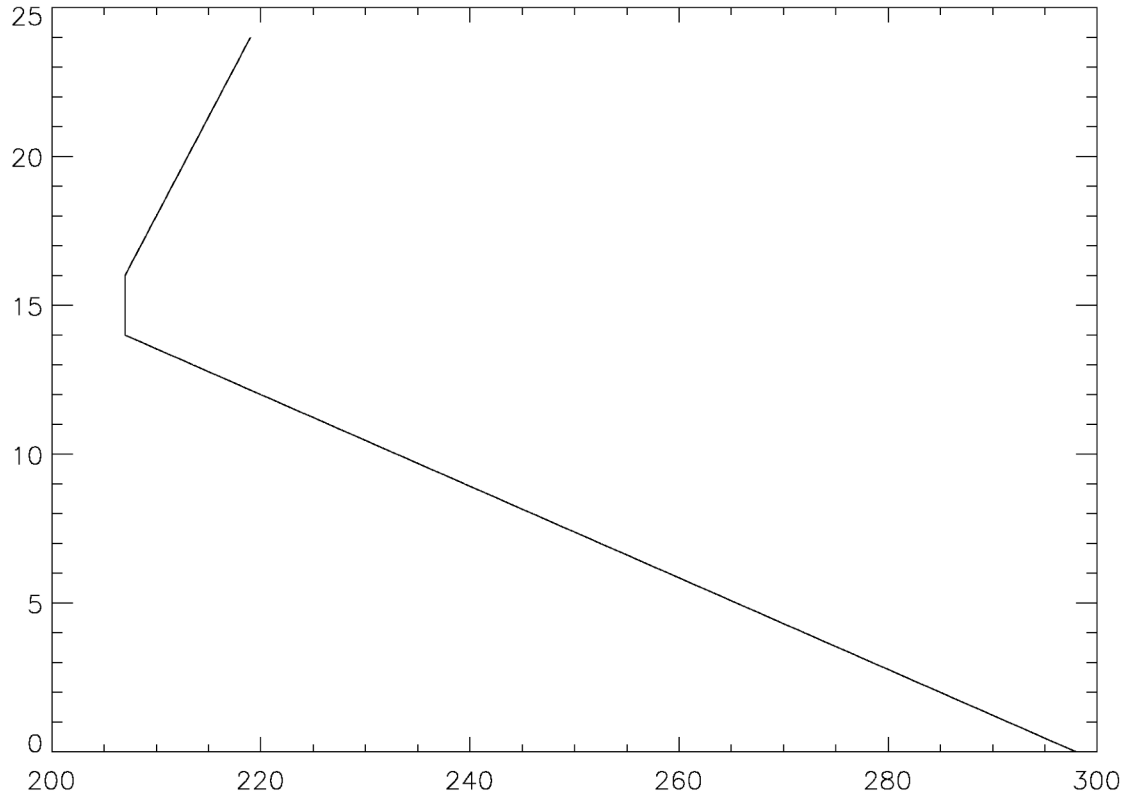


*Figure 1. Temperature versus altitude profile*

We define a water vapor profile.

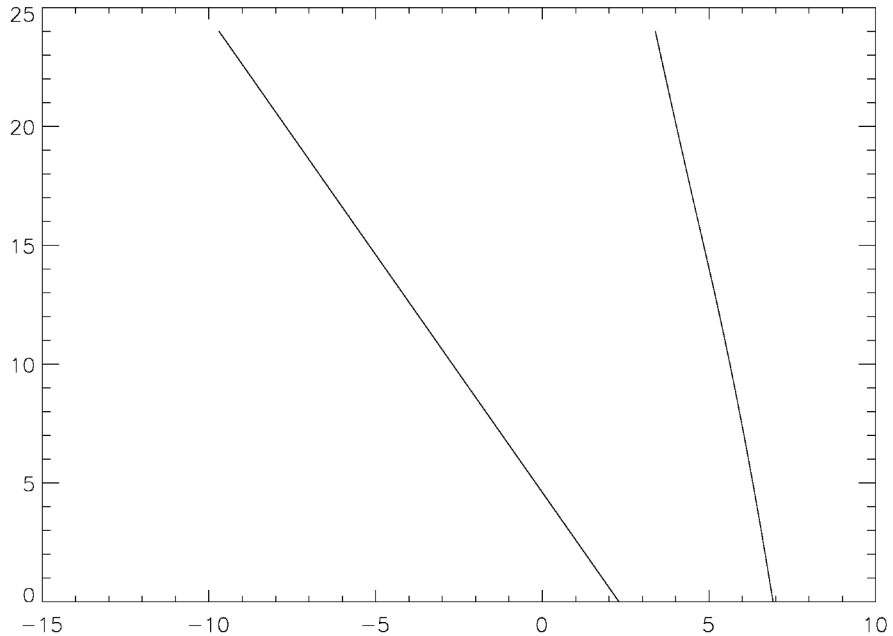


*Figure 2 natural log of the pressure (mb) and water vapor (mb) profiles used*

**LINE BROADENING**

As we know, the vertical information comes from the collisional broadening of the 183 GHz water line. As we have seen this broadening depends primarily of pressure but also on temperature.

In this case we will do things a bit more precisely than the simple 3 MHz/mb scaling that we have used thus far. We make the distinction between two sources of collisional broadening, heterogenous broadening (collisions with another type of molecule) and self-broadening (collisions with the identical molecule). Based on the HITRAN database, we calculate the collisional linewidth as

$$\nu_L = (T_{jpl}/T)^{expT} * (B_{air} * (P - P_w) + B_{h2o} * P_w) \quad (4)$$

where expT is the temperature scaling exponent which is 0.77 for the 183 GHz line. $B_{air}$ is 3.0029615 MHz/mb and $B_{h2o}$ is16.163870 MHz/mb and $T_{JPL}$ is 300 K, the reference temperature of the JPL database. Notice how large the water-water collisional broadening coefficient is indicating a very large collisional crossection consistent with the large permanent dipole moment of the water molecule.

**TEMPERATURE weighting functions**

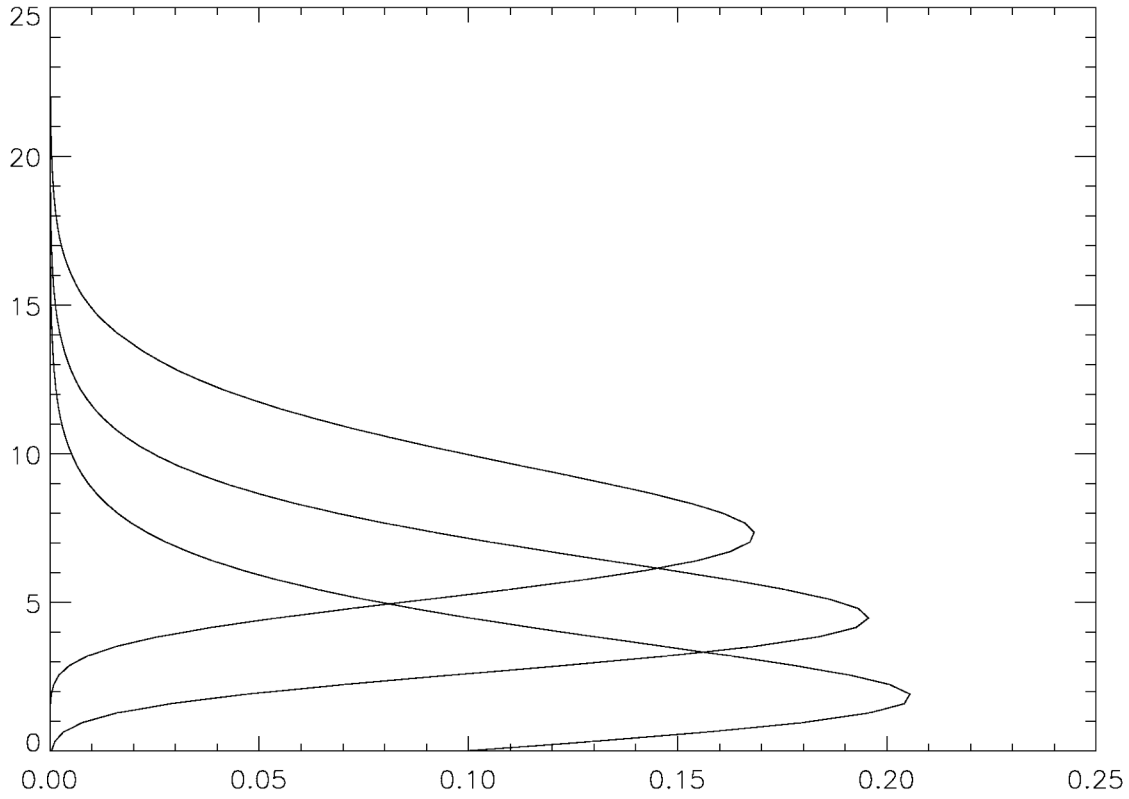


This gives some idea of the vertical information in the 3 AMSU-B 183 GHz channels.
***NOTE***: These are ***TEMPERATURE*** weighting functions that we are familiar with. However, here we are trying to solve for water vapor density, so the temperature weighting function tells only part of the story.

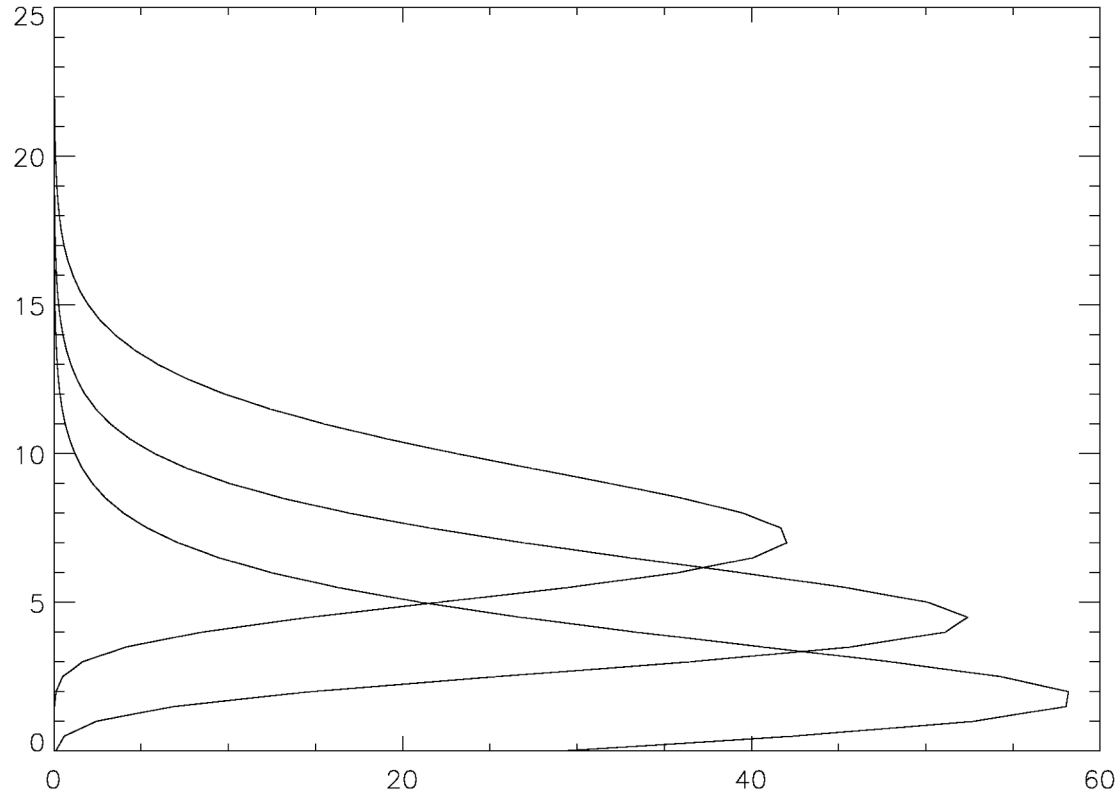


*Figure: Contribution function (T * weighting function) vs. altitude*

The three radiances (in K) are 243.57068 261.10683 258.53870
The third one would be higher but the third contribution function is chopped off by the surface and there is no surface emission (in the case we are considering).

**Error modeling**

We model both the measurement errors and the errors in the *apriori* state estimate as Gaussian. This defines the *apriori* state and measurement error covariances. It also defines the random noise that we add to the measurements in the simulations and the noise that we add to the true state to create the somewhat erroneous *apriori* state.

We add errors according to the Gaussian definitions

$$x_a = x + e_x \qquad y' = y + e_y \tag{5}$$

using a Gaussian random number generator.

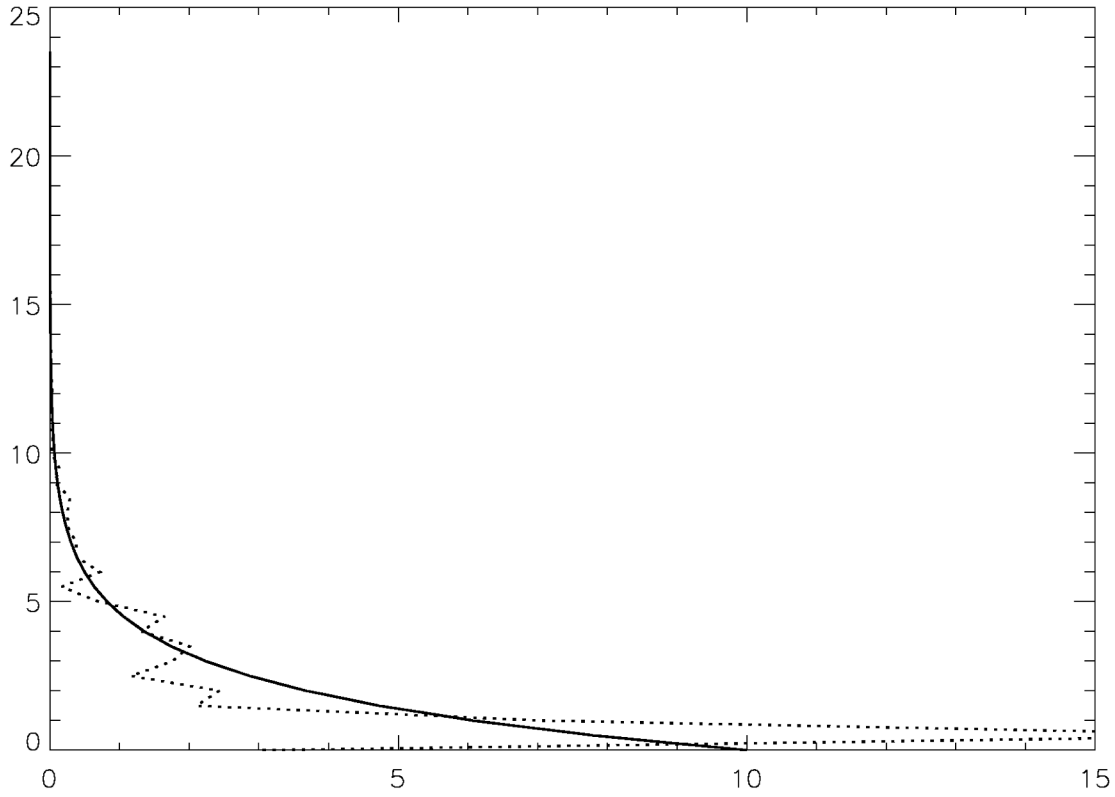


*Figure: One example of true profile of water vapor partial pressure, x, (solid line) and noisy estimate, $x_a$ (dotted line).*

**COVARIANCES**

For the covariance representing the uncertainty in the *apriori* state estimate, to simplify things, we make the off-diagonal, cross correlation terms of the state vector error covariance 0. We do the same for the measurement covariance making it diagonal meaning there is no correlation between the errors in the radiance measurements made at the different frequencies.

**dy/dx**

We calculate *dy*/*dx* numerically by slightly changing each element in the (*apriori*) state vector individually and then determining the resulting changes in the measurement vector. By doing this we fill in the dy/dx matrix.

In doing so we find that the numerically estimated dydx exhibits oscillations. These seem to be associated with the interpolation method to take the discrete number of vertical levels to perform the vertical integral to obtain the optical depth.

This is ok as long as the radiance calculation is consistent which it will be because we use the same route and interpolation scheme for all the forward radiance calculations including the derivative calculations.

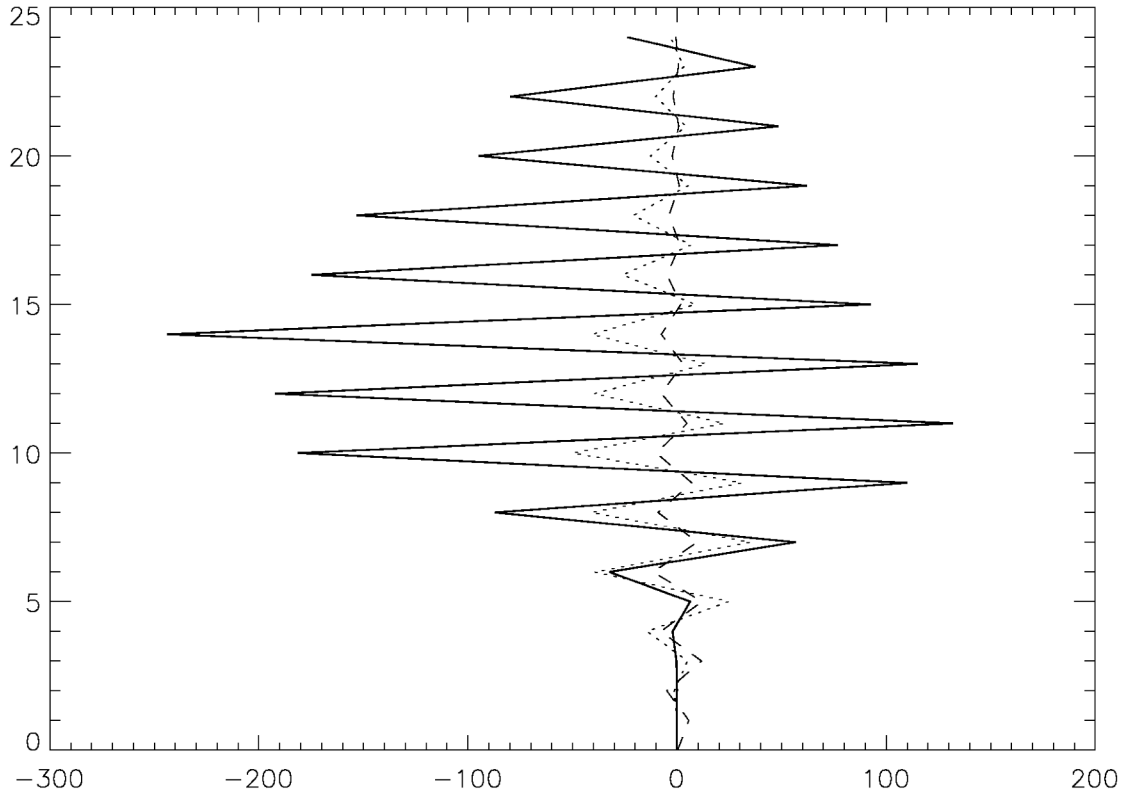


*Figure 3. The 3 dydx rows, one corresponding to each of the 3 AMSU measurement frequencies. The solid line is the row for the AMSU frequency closest to line center (184.31 GHz). The source of the oscillations may be numerical.*

**RESULTS**

Because the radiance calculations near the 183 GHz line are so nonlinear, we linearize around $y' = y[x_a]$, the set of radiances associated with the state, $x_a$. We therefore rewrite (1) as

$$\hat{x} = x_a + \left(K^T S_\varepsilon^{-1} K + S_a^{-1}\right)^{-1} K^T S_\varepsilon^{-1}\left(y - y\left[x_a\right]\right) \tag{1a}$$

The predicted errors are in the *posterior* error covariance whose inverse, $\hat{S}^{-1}$, is

$$\hat{S}^{-1} = K^T S_\varepsilon^{-1} K + S_a^{-1} \tag{6}$$

The following figure shows both the predicted error (the square root of the diagonal elements of $\hat{S}$) and the actual errors calculated via 4000 simulations.

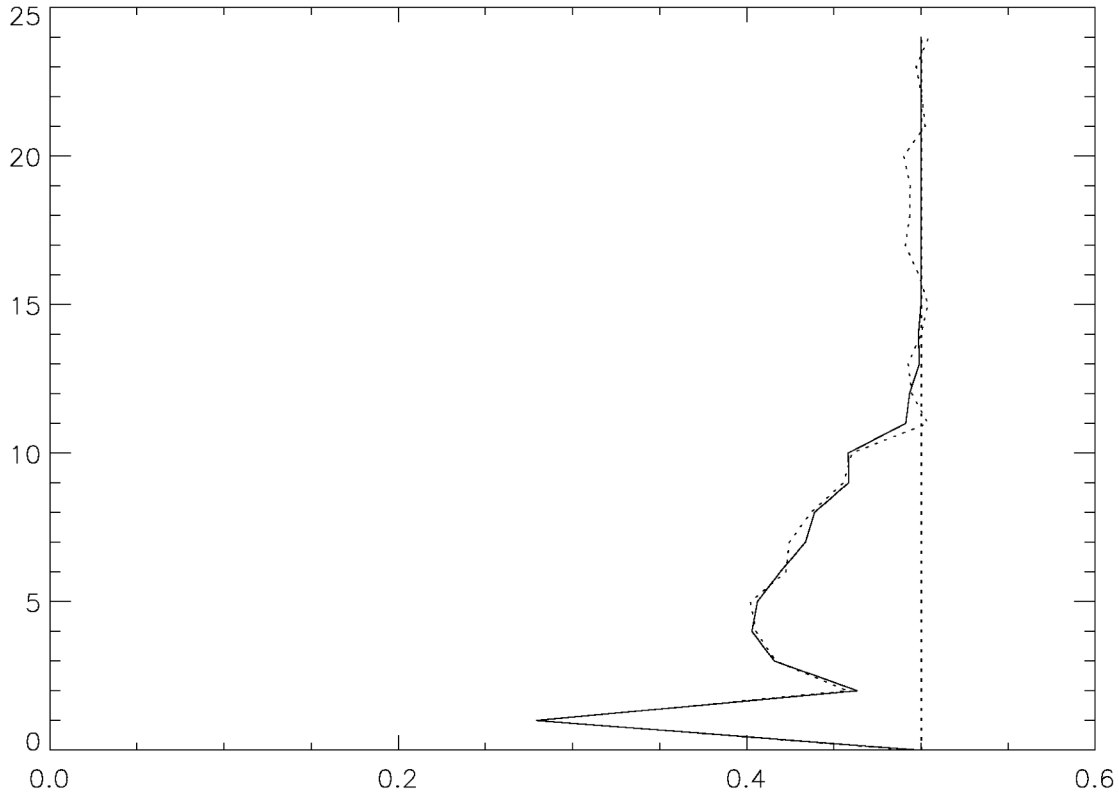


*Figure 4. Fractional errors in water vapor estimates with 1 km vertical spacing before and after adding the AMSU-B radiance measurements at 3 frequencies near the 183 GHz water line. X-axis is the fractional water vapor error. Y-axis is height in km. The 1-sigma radiance measurement error at each of the 3 frequencies is 0.5K. The apriori water vapor error is 50% (dotted line), with no correlation between the errors at different altitudes and 1 km vertical model resolution. Dotted line represents the 1-sigma errors in the apriori state estimate. The solid line is posterior state error covariance reflecting the improvement expected based on the AMSU measurements. The dashed lined is the actual state error based on 4000 simulations.*

**The state error Covariance before and after the radiance measurements are added.**

In our simulation we have assumed the *apriori* state vector errors are uncorrelated, an optimistic assumption. After the addition of the radiance measurements, the new and better *posterior* covariance now contains correlated errors between the different heights so the off-diagonal elements of the *posterior* covariance are non-zero. The greatest error correlation is introduced where the errors are most reduced.

IDL> print,Sa(0:4,0:4) ***APRIORI***

| | | | | |
|---|---|---|---|---|
| **25.000000** | 0.0000000 | 0.0000000 | 0.0000000 | 0.0000000 |
| 0.0000000 | **9.1969860** | 0.0000000 | 0.0000000 | 0.0000000 |
| 0.0000000 | 0.0000000 | **3.3833821** | 0.0000000 | 0.0000000 |

| | | | | |
|---|---|---|---|---|
| 0.0000000 | 0.0000000 | 0.0000000 | **1.2446767** | 0.0000000 |
| 0.0000000 | 0.0000000 | 0.0000000 | 0.0000000 | **0.45789097** |

IDL> print,Shat(0:4,0:4) ***POSTERIORI***

| | | | | |
|---|---|---|---|---|
| **24.935211** | -0.63996517 | 0.15628280 | -0.11085123 | -0.017393452 |
| -0.63996517 | **2.8665103** | 1.5139511 | -1.0528777 | -0.20917107 |
| 0.15628280 | 1.5139511 | **2.9094792** | 0.40439058 | -0.079856854 |
| -0.11085123 | -1.0528777 | 0.40439058 | **0.86070076** | 0.14105449 |
| -0.017393452 | -0.20917107 | -0.079856854 | 0.14105449 | **0.29733166** |

Note the reduction in the magnitudes of the diagonal elements indicating how adding the radiance information has reduced the water vapor uncertainties. Note that the off-diagonal elements in the ***posteriori*** elements are non-zero.

**Dependence on the vertical resolution of the state vector**

Higher vertical resolution models contain more information than low resolution models. Therefore, the added AMSU measurement information represents a smaller fraction of the total information for a high vertical resolution model than a lower vertical resolution model.

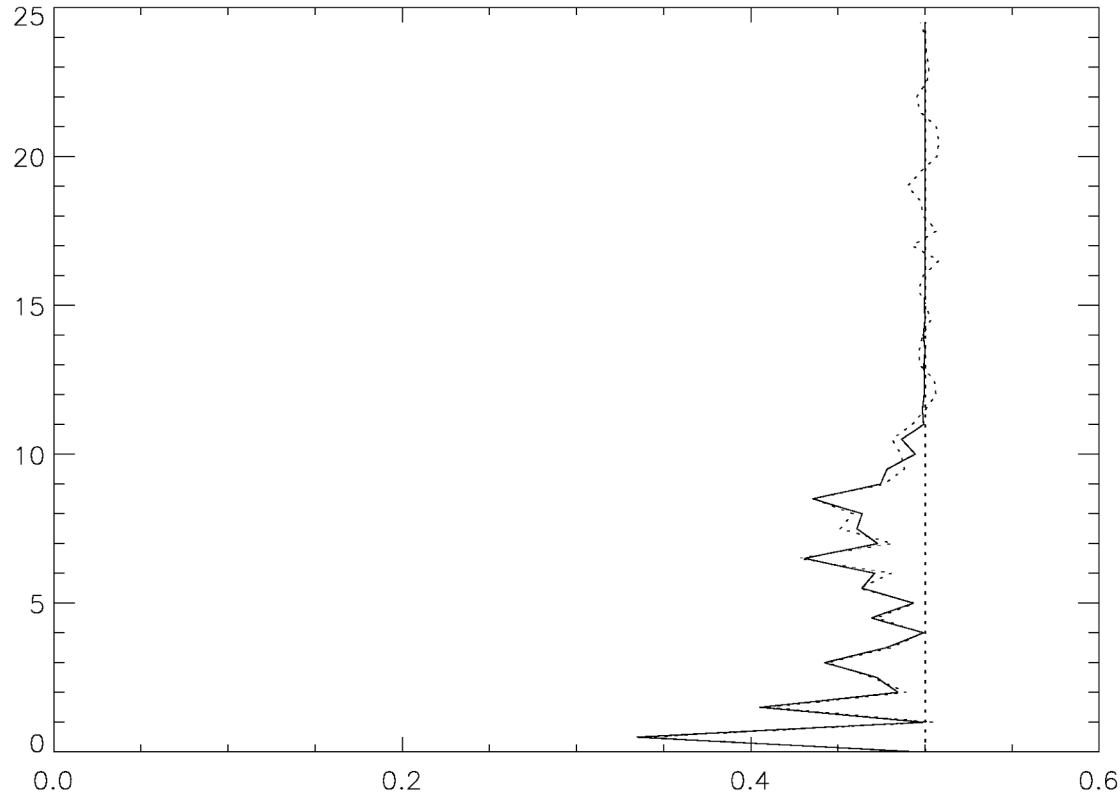


*Figure 5. Fractional errors in water vapor estimates spaced **0.5 km vertically** before and after adding the AMSU-B radiance measurements at 3 frequencies near the 183 GHz water line to an apriori estimate. X-axis is the fractional water vapor error. Y-axis is height in km. The 1-sigma radiance measurement error at each of the 3 frequencies is 0.5K. The apriori water vapor error is 50% (dotted line), with no correlation between the errors at different altitudes and 0.5 km*

*vertical model resolution. Dotted line represents the 1-sigma errors in the apriori state estimate. The solid line is posterior state error covariance reflecting the improvement expected based on the AMSU measurements. The dashed lined is the actual state error based on 4000 simulations.*

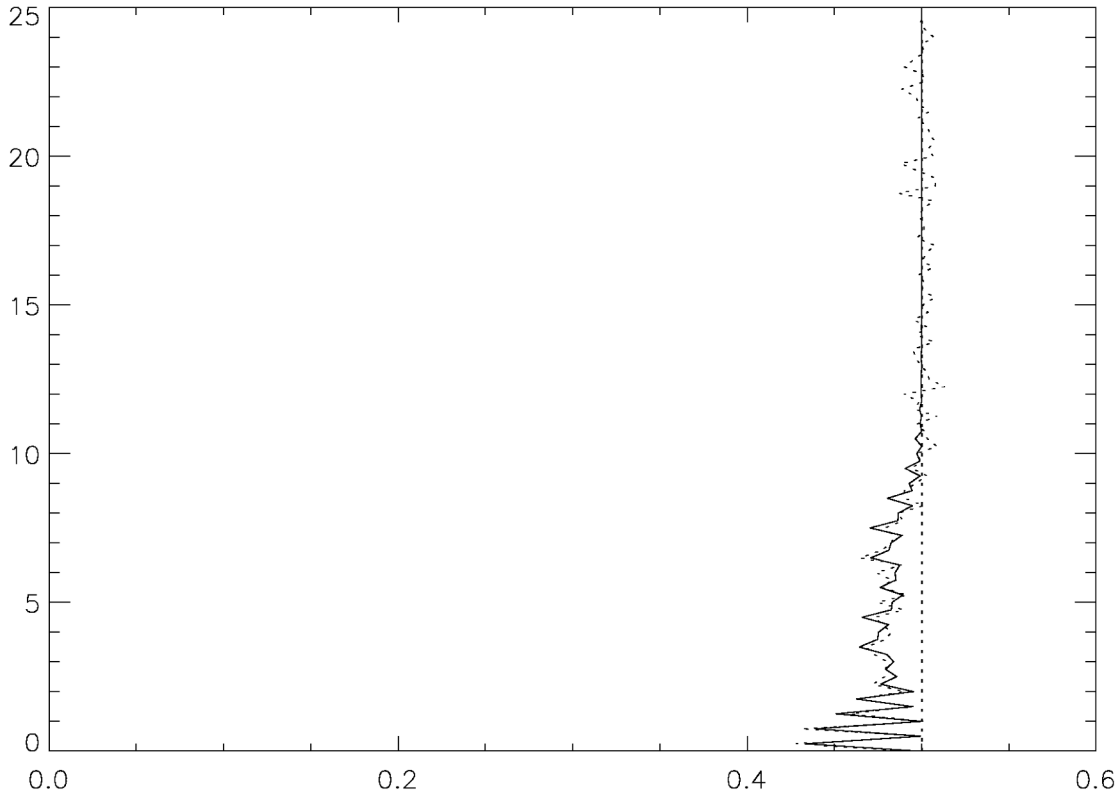


*Figure 6. Fractional errors in water vapor estimates spaced **0.25 km vertically** before and after adding the AMSU-B radiance measurements at 3 frequencies near the 183 GHz water line to an apriori estimate. Conditions are the same as previous figure except model vertical resolution is 0.25 km.*

**Information content**

In comparing Figures 4, 5 and 6, note how much the improvement has been reduced when the measurement information is spread over 2 and 4 times as many levels. In actuality, the extra information provided by the observations is pretty much the same in all 3 cases. The difference is that as the number of levels in the state vector increases, there are more ***degrees of freedom*** to solve for. However, the number of measurements remains the same. So while the number of degrees of freedom that can be solved for via the observations remains fixed because the number of measurements is fixed, the ***fraction*** of the number of degrees of freedom that can be solved for with the fixed number of observations decreases as the total degrees of freedom increases.

The number of degrees of freedom is initially the number of state variables which is given by adding the total ***normalized*** variance of the state vector. Normalized here means the variance of the uncertainty divided by the initial variance of uncertainty for each element in the state vector.

With accurate and independent measurements, the maximum reduction in the *apriori* degrees of freedom is one per measurement. This maximum can be achieved if the measurements really provide information independent from one another. The table below shows the reduction in the degrees of freedom for several different 183 GHz sensors.

| | # of state vector elements | # of obs | Reduction in initial degrees of freedom | % of potential improvement |
|---|---|---|---|---|
| AMSU-B | 25 | 3 | 3.00 | 100.0% |
| ATMS (5) | 25 | 5 | 4.87 | 97.4% |
| ATMS (6) | 25 | 6 | 5.77 | 96.2% |
| AMSU-B | 50 | 3 | 2.96 | 98.7% |
| ATMS (5) | 50 | 5 | 4.32 | 86.4% |
| ATMS (6) | 50 | 6 | 4.85 | 80.8% |
| 10 equal space frqs | 48 | 10 | 5.34 | 53.4% |
| AMSU-B | 75 | 3 | 2.97 | 98.9% |
| AMSU-B | 100 | 3 | 2.97 | 98.9% |
| ATMS (5) | 100 | 5 | 4.27 | 85.5% |
| ATMS (6) | 100 | 6 | 4.77 | 79.5% |

**ASSESSMENT OF 5 & 6 channel NPOESS Advanced Technology Microwave Sounder (ATMS)**

The National Polar-orbiting Operational Environment Satellite System (NPOESS) is supposed to be the grand unification of the U.S. civilian and military polar orbiting satellites. NPOESS has been VERY expensive and is over cost and behind schedule and some instruments have been dropped. I am not sure if ATMS is still on board.

Aircraft version of ATMS

| | Frequency | Bandwidth | Sensitivity | Est noise (Tsys= 2000K, 10 ms) |
|---|---|---|---|---|
| No. | Offset (MHz) | (MHz) | (RMS K) | K |
| 1 | ± 10000 | 3000 | 0.36 | 0.365 |
| 2 | ± 7000 | 2000 | 0.45 | 0.447 |
| 3 | ± 4500 | 2000 | 0.43 | 0.447 |
| 4 | ± 3000 | 1000 | 0.59 | 0.632 |
| 5 | ± 1800 | 1000 | 0.77 | 0.632 |
| 6 | ± 1000 | 500 | 1.39 | 0.894 |

183-GHz Spectrometer (LO = 183.31 GHz)from Leslie et al., 2003
6 channels each sampling both sides of the line

ATMS on NPOESS (missing the lowest frequency channel above)

| Channel | Center Frequency (GHz) | Maximum Bandwidth (GHz) | Temperature Sensitivity (K) NEΔT | Calibration Accuracy |
|---|---|---|---|---|
| 18 | 183.31 ± 7 | 2.0 | 0.8/0.47 | 2.0 |
| 19 | 183.31 ± 4.5 | 2.0 | 0.8/0.48 | 2.0 |
| 20 | 183.31 ± 3 | 1.0 | 0.8/0.57 | 2.0 |
| 21 | 183.31 ± 1.8 | 1.0 | 0.8/0.58 | 2.0 |
| 22 | 183.31 ± 1.0 | 0.5 | 0.8/0.75 | 2.0 |

The stated RMS noise is quite small
*sigma* = $T_{sys}$(*SSB*)/(*BW***t*)**0.5

where *SSB* equals single side band, *BW* = bandwidth (e.g. channel width) and *t* = integration time. Plugging in a $T_{sys}$ of 2000K and an integration time of 0.01 seconds we get numbers similar to the stated numbers. So they are believable. Note that the fact that they quote these values as an RMS means that these include any biases in the instrument which may or may not actually be achievable on orbit.

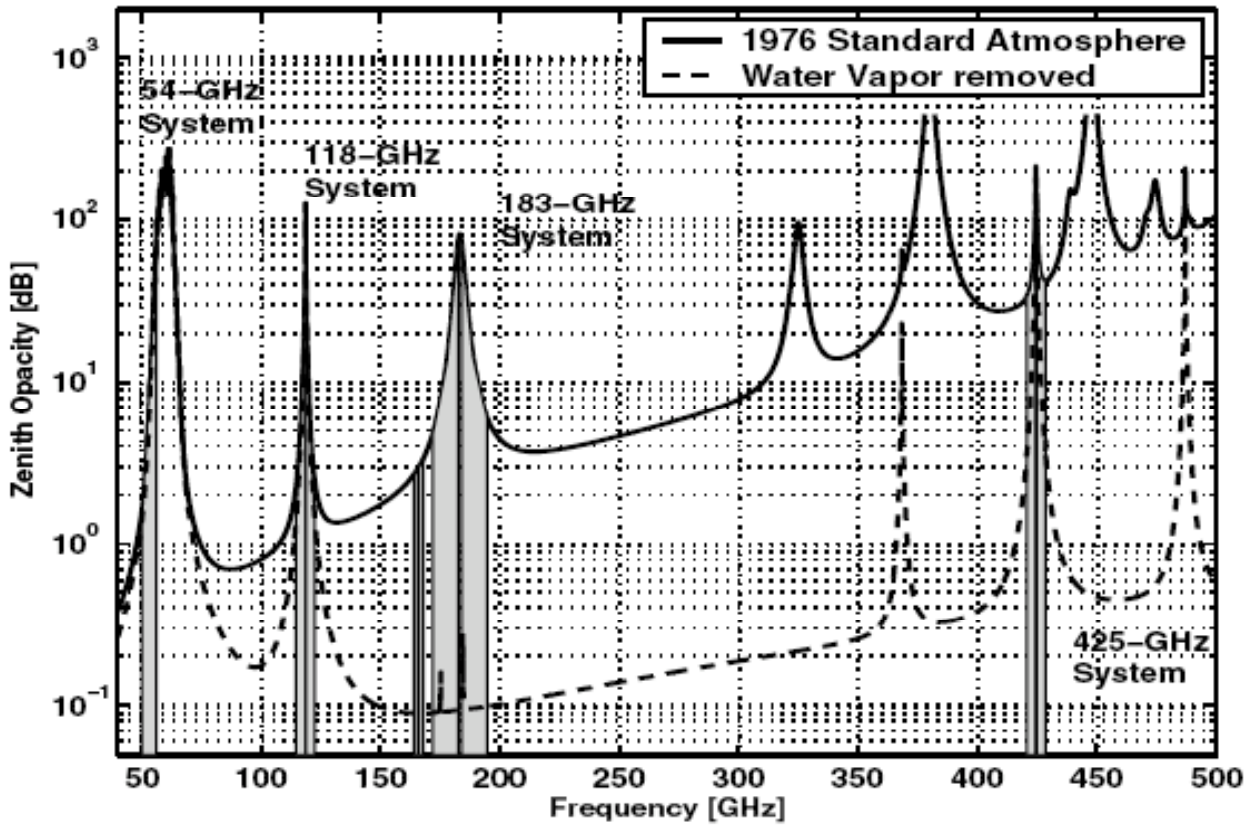


*Spectrum of the airborne version of the NPOESS ATMS*

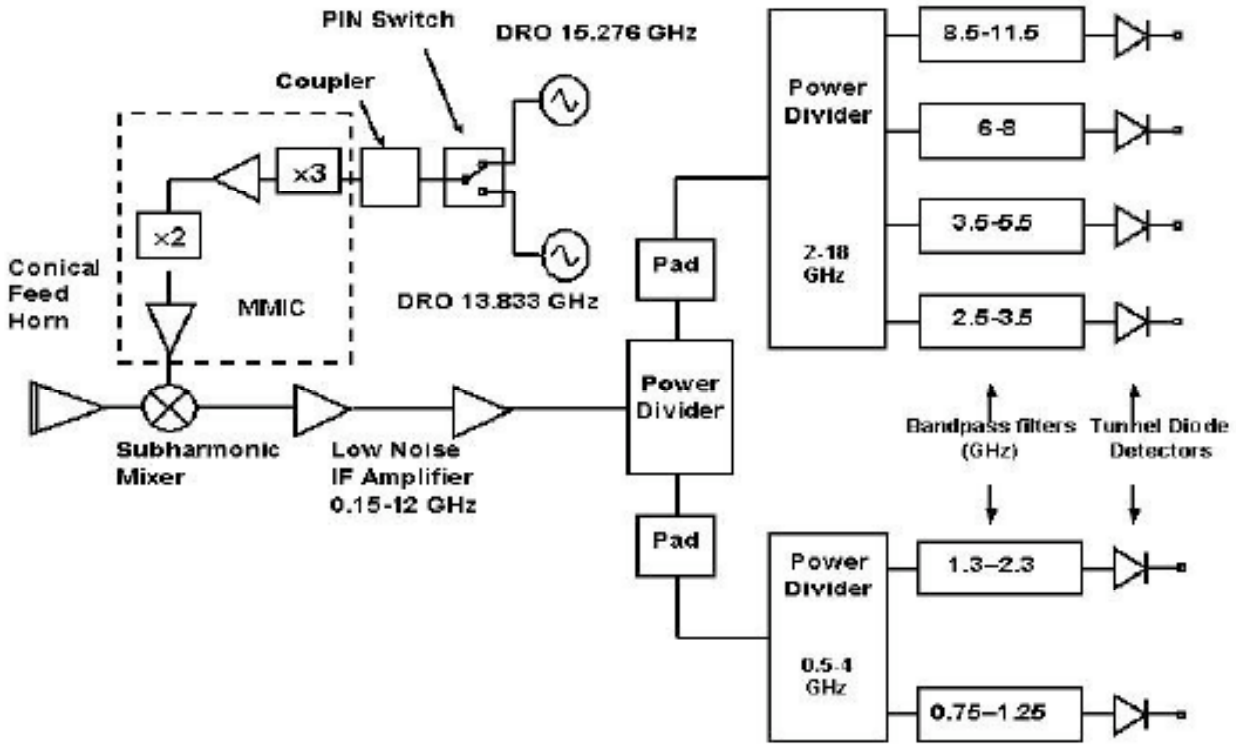


*Figure . Block Diagram of airborne version of the NPOESS ATMS*

***Performance***

- Not bad in our estimate: 6 meas reduces 1 km degrees of freedom by 5.77
- Note that our estimate does not include water vapor continuum and problems associated with uncertainties in atmospheric temperature, surface emissivity, clouds and rain.
- Also the vertical information is actually somewhat less than what has been assumed because the bandwidths of the 6 channels are so wide.
- There is also not much room for further improvement around the 183 GHz line. One cannot add many more frequencies because bandwidths are so wide presumably to maximize SNR. The airborne version, uses 11,500 MHz of signal range and 9,500 MHz of bandwidth. So there is only 2,000 MHz or 15% of the frequency range that is not sensed. Also the noise is quite low even with short integration times so even with longer averaging from geosync orbits, the performance will not improve much. The impact is limited by the vertical information.

**PROBLEMS with Gaussian version of Bayesian approach:**

The combined apriori and measurement approach yields the optimum solution ***as long as the assumptions are correct***.

However, the uncertainty in the *apriori* estimate is probably not Gaussian.

Assumes the first guess is "good" which for water vapor it may not be.

Assumes biases are zero in *apriori* and therefore the model.

Assumes biases are zero in measurements

In NWP data assimilation, the reality is that the observations are sometimes de-weighted to produce better forecasts as a result of model flaws because observations may expose errors that are otherwise masked by removing some error cancellation in the model being used.
If we fully understood the model errors, we wouldn't be wondering about the accuracy of climate predictions.

**Additional cases:**
7 freq: 183.31d0, 183.81d0, 184.31d0, 185.31d0, 186.31d0, 188.31d0, 190.31d0 GHz
offset 0 0.5 1.0 2.0 3.0 5.0 7.0 GHz

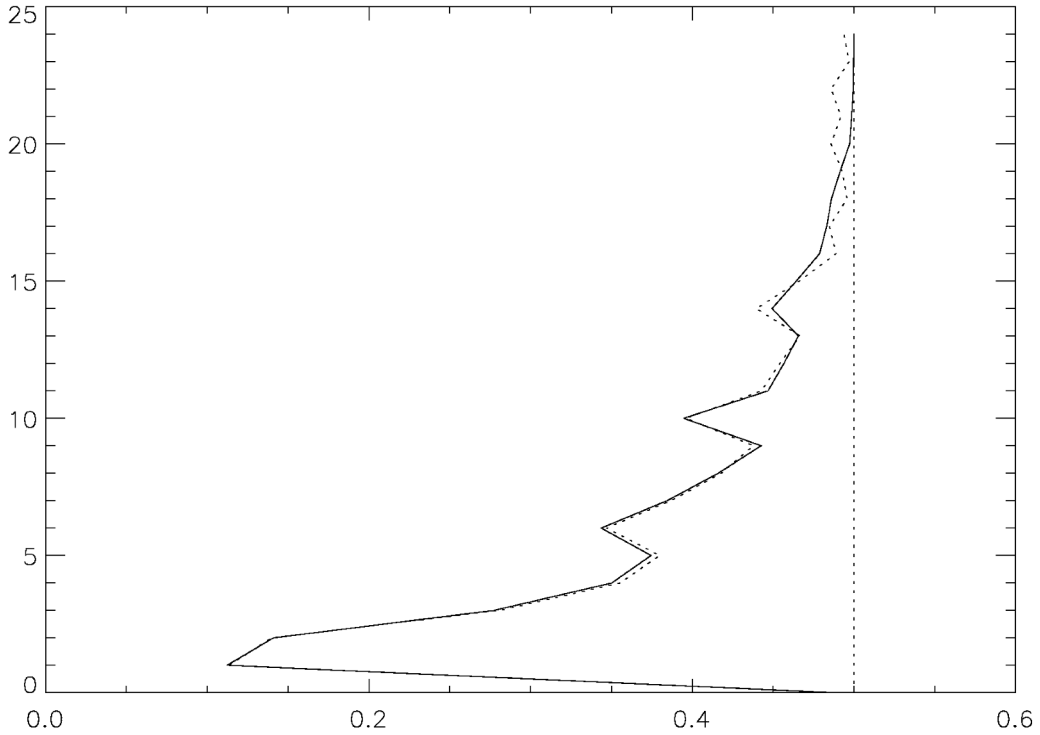


*7 frequencies, 0.5K errors each, apriori model error 50%, no correlation, 1 km vertical model resolution. Solid line is predicted improvement. Dotted lined is observed improvement based on 4000 simulations.*

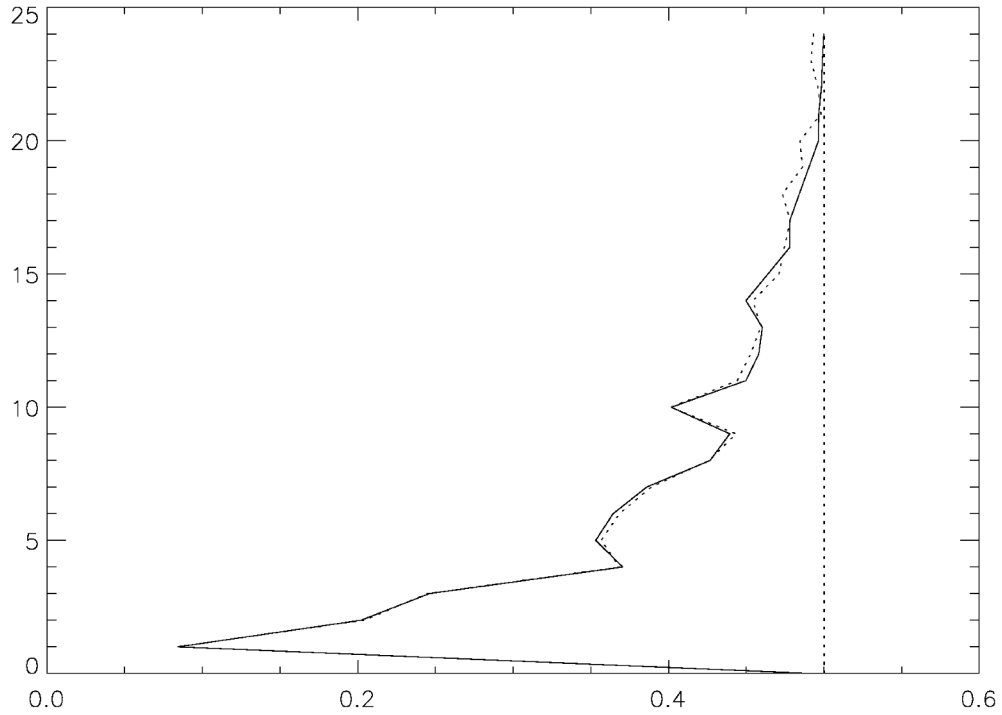


*7 frequencies, 0.5K errors each, apriori model error 50%, no correlation, 0.5 km vertical model resolution. Solid line is predicted improvement. Dotted lined is observed improvement based on 4000 simulations.*

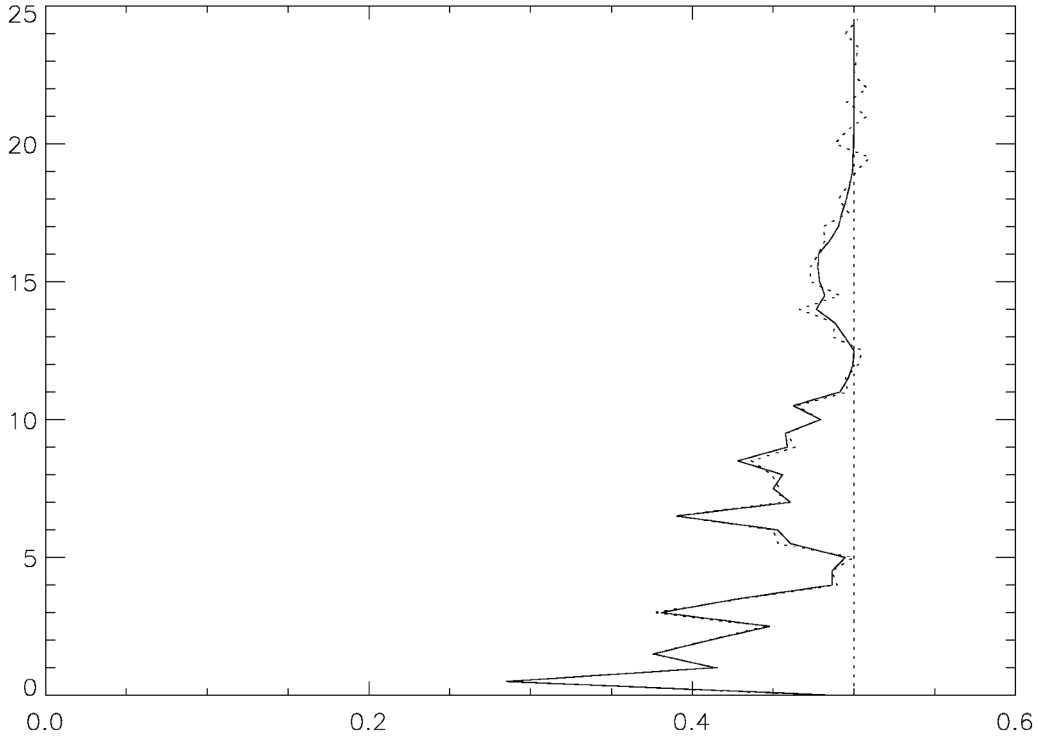


*7 frequencies, 0.5K errors each, apriori model error 50%, no correlation, 0.25 km vertical model resolution. Solid line is predicted improvement. Dotted lined is observed improvement based on 4000 simulations.*

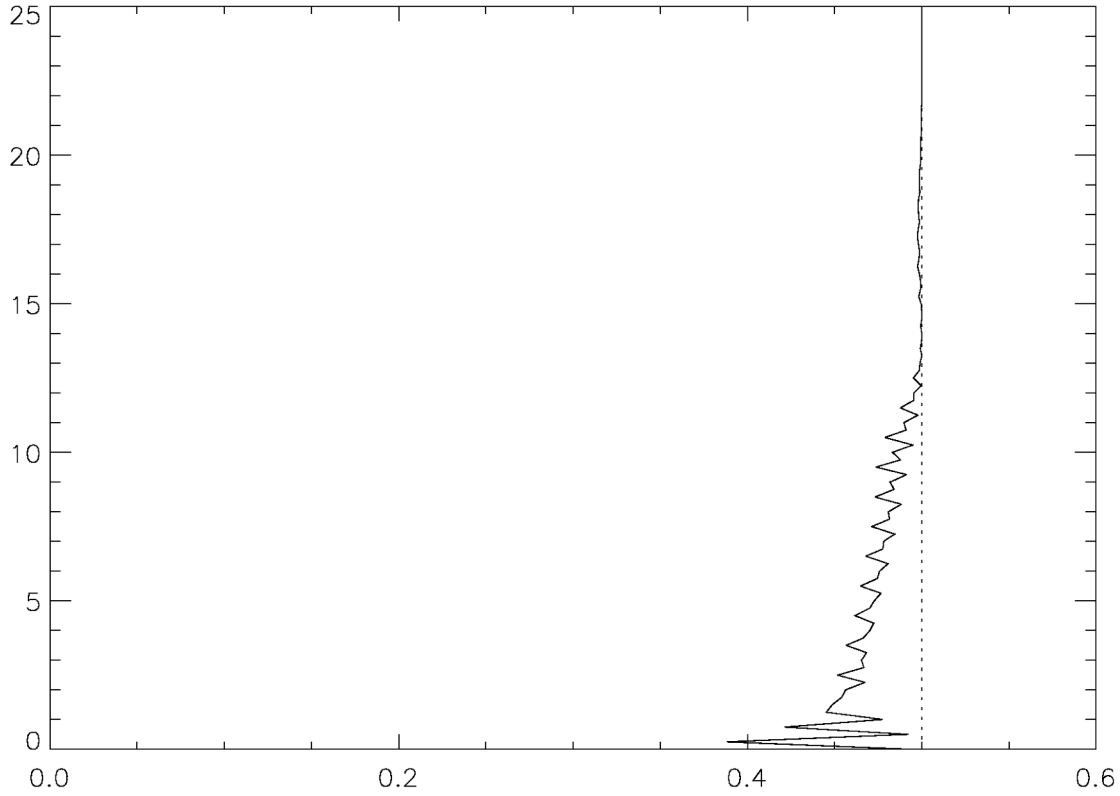


**References**

R. V. Leslie, W. J. Blackwell, P. W. Rosenkranz, and D. H. Staelin (2003), 183-GHz and 425-GHz Passive Microwave Spectrometers on the NPOESS Aircraft Sounder Testbed-Microwave (NAST-M), Massachusetts Institute of Technology, 77 Massachusetts Avenue (Room 26-341), Cambridge, MA 02139-4307, tel: 617-253-3711; fax: 617-258-7864; e-mail: staelin@mit.edu, 0-7803-7929-2/03/$17.00 (C) 2003 IEEE, p. 506